Pyykkönen, Ville A.J.; Peotta, Sebastiano; Törmä, Päivi

# Suppression of Nonequilibrium Quasiparticle Transport in Flat-Band Superconductors

*Published in:*
Physical Review Letters

*DOI:*
10.1103/PhysRevLett.130.216003

Published: 26/05/2023

*Document Version*
Publisher's PDF, also known as Version of record

*Please cite the original version:*
Pyykkönen, V. A. J., Peotta, S., & Törmä, P. (2023). Suppression of Nonequilibrium Quasiparticle Transport in Flat-Band Superconductors. *Physical Review Letters*, *130*(21), 1-7. Article 216003.
https://doi.org/10.1103/PhysRevLett.130.216003

Editors' Suggestion | Featured in Physics

# Suppression of Nonequilibrium Quasiparticle Transport in Flat-Band Superconductors

Ville A. J. Pyykkönen, Sebastiano Peotta, and Päivi Törmä*
*Department of Applied Physics, Aalto University School of Science, FI-00076 Aalto, Finland*

(Received 17 November 2022; accepted 13 April 2023; published 25 May 2023)

We study nonequilibrium transport through a superconducting flat-band lattice in a two-terminal setup with the Schwinger-Keldysh method. We find that quasiparticle transport is suppressed and coherent pair transport dominates. For superconducting leads, the ac supercurrent overcomes the dc current, which relies on multiple Andreev reflections. With normal-normal and normal-superconducting leads, the Andreev reflection and normal currents vanish. Flat-band superconductivity is, thus, promising not only for high critical temperatures, but also for suppressing unwanted quasiparticle processes.

DOI: 10.1103/PhysRevLett.130.216003

The destructive interference of waves scattered from a periodic potential can lead to disorder-free localization, which manifests as the vanishing of the energy width of a band in the band structure [1]. Currently, an important goal is to engineer materials in which these so-called flat bands occur, as this generally allows one to enter a strongly correlated regime with emerging exotic phases. Well-known instances of this general picture are the fractional quantum Hall effect and Chern insulators [2,3], and, more recently, twisted bilayer graphene and similar moiré materials [4–9], which are built by stacking and twisting atomic layers with various compositions.

The discovery of superconductivity at the "magic" angle in twisted bilayer graphene (TBG) has amplified the interest in the problem of superconductivity in the flat-band limit and its competition with other phases, such as correlated insulators [4,7,10]. This is a challenging problem due to strong correlations; nevertheless, it has received a lot of attention [11–29], and even exact results can be derived for the ground state and excitations under some conditions [30,31]. Moreover, it was shown that superconductivity in flat bands originates from quantum geometry and topology [11,13,15,23]. Flat-band superconductivity is particularly promising as a route for higher-temperature superconductivity, as the critical temperature is linearly proportional to the interaction energy [32–34], while it is exponentially suppressed for weak coupling in the case of a dispersive band [35].

A major open question is the transport properties of a superconducting state in the flat-band limit. Transport in superconductors and superconductive weak links typically includes nondissipative ac and dc supercurrents, as well as dissipative transport involving fermionic quasiparticles [36]. It has been theoretically shown that equilibrium dc supercurrents are possible in flat bands [10,11,22], but, otherwise, little is known about transport. In certain highly symmetric flat-band systems, single particles remain localized due to local conserved quantities [37], and quasiparticle excitations have a flat dispersion [31], while pairs can be mobile. These equilibrium results on infinite bulk systems hint that flat-band transport could show unique features also in out-of-equilibrium situations, i.e., under voltage or current bias, and in the presence of interfaces. In this work, we focus on *out-of-equilibrium* transport in a lattice model with a flat band in which superconductivity arises due to a local attractive interaction. We find that the nondissipative supercurrent, the current carried coherently by highly mobile Cooper pairs, dominates over the dissipative current involving quasiparticles. The absence of quasiparticle transport and dissipation suggests flat-band superconductors as remarkably promising building blocks for quantum devices.

We address the nonequilibrium transport properties by using the two-terminal setup depicted in Fig. 1(a), where also the notation and the model flat-band system, the sawtooth lattice, are presented. In the setup, a middle structure ($M$) is connected via leads to two reservoirs, left ($L$) and right ($R$), respectively. The leads can be either normally conducting ($N$) or superconducting ($S$), enabling three different lead configurations: normal-normal (NN), normal-superconducting (NS), and superconducting-superconducting (SS).

The setup is modeled using the following tight-binding Hamiltonian with an Hubbard interaction term:

$$\hat{H} = \sum_{\alpha i \beta j, \sigma} T_{\alpha i, \beta j} \hat{c}^{\dagger}_{\alpha i \sigma} \hat{c}_{\beta j \sigma} + \sum_{\alpha i} U_{\alpha i} \hat{c}^{\dagger}_{\alpha i \uparrow} \hat{c}^{\dagger}_{\alpha i \downarrow} \hat{c}_{\alpha i \downarrow} \hat{c}_{\alpha i \uparrow}, \quad (1)$$

where $T_{\alpha i, \beta j}$ is the single-particle Hamiltonian with $\alpha, \beta \in \{L, R, M\}$ labeling different parts of the system, $i$ and $j$ are site indices, $\sigma = \{\uparrow, \downarrow\}$ is the spin index, and $U_{\alpha i} \leq 0$ is the attractive interaction strength. The graph in Fig. 1(a) shows the single-particle tight-binding parameters of the model. Specifically, the single-particle Hamiltonian can be divided as $\hat{H}_0 = \hat{H}_L + \hat{H}_R + \hat{H}_M + \hat{H}_{\text{contact}}$, where $\hat{H}_L$, $\hat{H}_R$, and

 

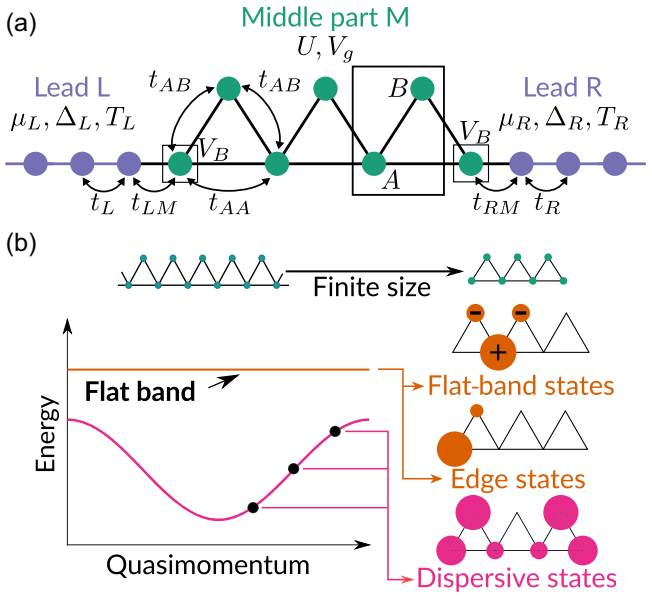


FIG. 1. The model used in the calculations. (a) The two-terminal setup with a piece of sawtooth lattice (middle part $M$) connected to two leads modeled by semi-infinite chains, labeled left ($L$) and right ($R$). The figure also highlights the sawtooth lattice unit cell which has two sites, labeled $A$ and $B$, and the edge sites. The graph corresponds to the tight-binding model hopping amplitudes. Here, $U < 0$, $V_g$, and $V_B$ correspond to interaction strength, gate potential, and boundary potential, respectively, in the middle part, and $\mu_{L/R}$, $\Delta_{L/R}$, and $T_{L/R}$ are the chemical potential, superconducting order parameter, and temperature of the left and right leads, respectively. (b) Correspondence between the sawtooth lattice and the truncated piece. The flat-band states of the infinite system are also present in the finite size system, since the destructive interference remains. At the edges, the flat-band states are changed to edge states, which we tune to degeneracy with the flat-band states by a boundary potential. The dispersive band corresponds to the dispersive states.

$\hat{H}_M$ are the Hamiltonians of the left lead ($L$), right lead ($R$), and the middle part ($M$) in between the leads, respectively, and $\hat{H}_{\text{contact}}$ connects them together. The tight-binding matrices corresponding to the lead Hamiltonians $\hat{H}_L$ and $\hat{H}_R$ are given by $T_{L/Ri,L/Rj} = -\delta_{ij}\mu_{L/R} - \delta_{j,i\pm1}t_{L/R}$, where $\mu_{L/R}$ are the chemical potentials of the respective leads and $t_{L/R}$ are their hopping amplitudes. The tight-binding matrix related to the middle part Hamiltonian $\hat{H}_M$ is given by $T_{Mi,Mj} = \delta_{ij}(-V_g + V_B\delta_{j,\text{edge}}) - t_{M,ij}$, where $V_g$ is the gate potential used to control the filling of the middle part states, $t_{M,ij}$ is the model-specific hopping matrix given by the graph in Fig. 1(a), and $V_B$ is a boundary potential at the edge sites used to control the edge state energies [22]. The contact Hamiltonian $\hat{H}_{\text{contact}}$ corresponds to $T_{Mi,L/Rj} = T_{L/Rj,Mi} = -t_{L/R,M}\delta_{i,\text{edge}}\delta_{j,0}$, $t_{L/R,M}$ being the respective hopping amplitudes.

As a specific example of a system with a flat band, we look at the sawtooth ladder shown in Fig. 1(a). When the hopping amplitudes satisfy the condition $t_{AB} = \sqrt{2}t_{AA}$, the upper band becomes flat, as shown in Fig. 1(b), since it is composed of localized V-shaped states. We look at a finite segment of the sawtooth ladder with $N$ unit cells and an additional $A$ site. An earlier study [22] has shown that flat-band equilibrium transport, i.e., the dc Josephson effect, is possible through a finite segment of the sawtooth ladder, while no current is seen in the flat band in the absence of interactions. As indicated in Fig. 1(b), the system has $N-1$ flat-band states, $N$ dispersive band states, and two edge states exponentially localized to the edges, which result from the edge flat-band states due to the absence of one of the $B$ sites. The edge states can be made degenerate with the flat-band states by setting the boundary potential at the edge sites to $V_B = t_{AA}$. This has also the effect of perfectly localizing the edge states to the edge $A$ and $B$ sites [22].

We enter the out-of-equilibrium regime by applying a chemical potential bias $V = \mu_L - \mu_R$. The current is computed with the nonequilibrium Green's functions [38,39] method, also known as the Schwinger-Keldysh [40,41] or Kadanoff-Baym [42] method. We evaluate the current at the left lead $I_L = 4\text{Im}(t_{LM}\langle\hat{c}^\dagger_{L,0\uparrow}\hat{c}_{M,\text{left edge}\uparrow}\rangle)$, which takes into account also the down-spin current by an additional factor of 2. The details of the method are given in Supplemental Material [43]. Similar approaches have been used to study, for instance, point contacts [52], quantum dots [53], magic-angle TBG [54], and many other systems [55] in a two-terminal setup. We limit our attention to the stationary state solutions, where we assume that the initial correlations and the transient effects have vanished.

We treat the Hubbard interaction with a self-consistent mean-field approximation: We take both the superconducting order parameter and the Hartree potential into account. The mean-field approximation has been shown to be an accurate description of flat-band superconductivity at equilibrium in a number of works [12,13,24,25,30]. The mean-field Hamiltonian is compactly written using the Nambu spinors $\hat{d}_{\alpha i} = (\hat{c}_{\alpha i\uparrow}, \hat{c}^\dagger_{\alpha i\downarrow})^T$ as

$$\hat{H}_{MF}(t) = \sum_{\alpha i,\beta j}\hat{d}^\dagger_{\alpha i}\begin{pmatrix} T_{\alpha i,\beta j} + V_{H,\alpha i}(t)\delta_{\alpha i,\beta j} & \Delta_{\alpha i}(t)\delta_{\alpha i,\beta j} \\ \Delta_{\alpha i}(t)^*\delta_{\alpha i,\beta j} & -T^*_{\alpha i,\beta j} - V_{H,\alpha i}(t)\delta_{\alpha i,\beta j}\end{pmatrix}\hat{d}_{\beta j}, \tag{2}$$

where $\Delta_{\alpha i}(t)$ and $V_{H,\alpha i}(t)$ are the superconducting order parameter and the Hartree potential, respectively, which are determined self-consistently for the middle part utilizing the equations $\Delta_{\alpha i} = U_{\alpha i}\langle \hat{c}_{\alpha i\downarrow}\hat{c}_{\alpha i\uparrow}\rangle$ and $V_{H,\alpha i} = U_{\alpha i}\langle \hat{c}^{\dagger}_{\alpha i\uparrow}\hat{c}_{\alpha i\uparrow}\rangle$. The leads are considered with a constant, uniform order parameter, and their respective Hartree potentials are absorbed into their chemical potentials $\mu_{L/R}$. As the notation reminds, the time-independent Hubbard interaction may result in a time-dependent mean-field theory at nonequilibrium conditions, which is the case now for the SS junctions even in the stationary state. In the time-periodic situation, we include the harmonics coefficients until they are within the self-consistent accuracy. In addition, we make frequency cutoffs to make the calculation feasible. The self-consistency is determined using the relative maximum error metric, and the accuracy we demand is $10^{-5}$.

Current-carrying processes can be classified into two categories within the limits of the mean-field theory: pure coherent pair transport and processes involving quasiparticle transport. Incoherent pair transport and processes involving more complicated $n$-body states are not included in our approach. With one or both of the leads being normal, only the quasiparticle-related processes are possible, but with the superconducting leads also the coherent pair transport may contribute.

Quasiparticle transport can occur through a channel by a combination of direct transmissions, branch-crossing transmissions, reflections, and Andreev reflections (AR) [56,57]. In the case of the NS and SS junctions, since there are no quasiparticle states available within the superconducting gap, an AR may occur [58] where a particle is reflected as a hole of the opposite spin. In the process, a Cooper pair is transmitted to the superconducting reservoir (or removed in the opposite process). In the case of an SS junction, quasiparticle transport for a bias smaller than the superconducting gaps is enabled by the multiple AR (MAR), where AR occurs multiple times between the leads until the quasiparticle escapes [56,59]. Also, the branch-crossing transmission from a quasiparticle into its time-reversed counterpart on the other side may occur at a bias larger than the superconducting gap; however, these are not important in our work.

Coherent Cooper pair transport, that is, the Josephson effect, occurs between superconducting reservoirs with relative superconducting order parameter phase difference [36,60]. Importantly, the order parameter has the time dependence $\Delta = |\Delta|\exp[i(\phi_0 + 2E_F t)]$, where $E_F$ is the Fermi energy [57]. Therefore, with a constant bias $V$, the superconducting phase difference $\phi$ evolves over time $\phi(t) = \phi_0 + 2Vt$, leading to an alternating current, i.e., the ac Josephson effect. In other words, two superconductors with a relative bias is an inherently time-dependent system having no time-independent steady-state solution.

The ac Josephson effect is a coherent and nondissipative phenomenon due to the Cooper pairs only. The AR and MAR are coherent processes that involve both Cooper pairs and quasiparticles and, due to the latter, are dissipative. For the sake of brevity, in the following, we refer to the ac Josephson effect as coherent pair transport or process and AR (MAR) as quasiparticle transport (process).

First, we look at transport through an SS junction, since it provides the clearest connection to the known equilibrium transport features with a similar setup, presented in Ref. [22]. It also allows a direct comparison between the pair and the quasiparticle contributions, namely, the ac Josephson effect and the MAR. As mentioned above, the stationary solution of an SS junction at a time-constant bias $V$ is time periodic with the period of $\tau = \pi/V$ (in units where $\hbar = e = 1$). Figure 2 presents the dc component and the first harmonic ac sine component of the current through the sawtooth lattice at a constant bias $V$ and varying gate potential $V_g$, which controls the filling. The two flat-band states and the two edge states lie at the gate potential $V_g = 2t_{AA}$, and the three dispersive band states are between $V_g = -4t_{AA}$ and $V_g = 0$. The states corresponding to the dispersive band exhibit a finite ac current, where the amplitude variation shows Fano-resonance-type behavior. The dc component, which corresponds to quasiparticle MAR processes, exhibits current peaks related to the

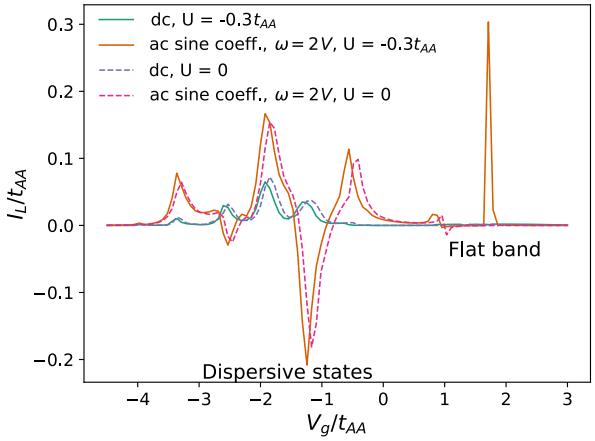


FIG. 2. Left lead current $I_L$ through the sawtooth lattice with three unit cells and an additional site between two superconducting leads at a varying gate potential $V_g$ with a constant bias $V$. The parameters are $U = -0.3t_{AA}$, $V = 0.5t_{AA}$, $t_{LS} = t_{RS} = 5.3t_{AA}$, $\Delta_{L/R} = t_{AA}$, and $T_{L/R} = 0$, and the leads are in the wideband limit with $t_{L/R} = 30t_{AA}$. The dc current is dominated by the quasiparticle MAR processes, which are finite around the dispersive states located at gate potential $-4 < V_g/t_{AA} < 0$, where there are current peaks. The quasiparticle current around the flat band, located around $V_g/t_{AA} = 2$, vanishes. In strong contrast, the ac Josephson current, that is, the ac sine component of the current at the Josephson frequency $2V$, has, in addition to the peaks at the dispersive states, a prominent peak corresponding to the flat-band states.

dispersive states. There are more peaks than the corresponding three dispersive states: MAR depends on the particular path in energy a quasiparticle passes [53], resulting in sensitivity to the gate potential $V_g$ and many local maxima. In general, the dispersive band acts as a point-contact channel in an expected manner, and having interactions in the middle part ($U \neq 0$) has no qualitative effect. The flat-band states, in contrast, have no current in the zero interaction case, but the ac sine component has a large amplitude in the presence of interactions (and superconductivity) in the middle part. Most remarkably, in strong contrast to the ac component, the flat-band dc current vanishes even at finite interaction. This indicates that the quasiparticle transport is quenched.

We have also considered the NN and NS lead configuration transport through a flat band. The results are shown in Fig. 3. The dispersive states in the NN case correspond to clearly defined peaks when their filling is varied by the gate potential $V_g$. The Andreev reflection in the NS case varies less smoothly, with sharper peaks around the dispersive region. However, the flat-band current is small with both configurations, similarly to the MAR-dominated dc transport in the SS junction. The current in the NN and NS cases is related to quasiparticle current, as, in terms of the

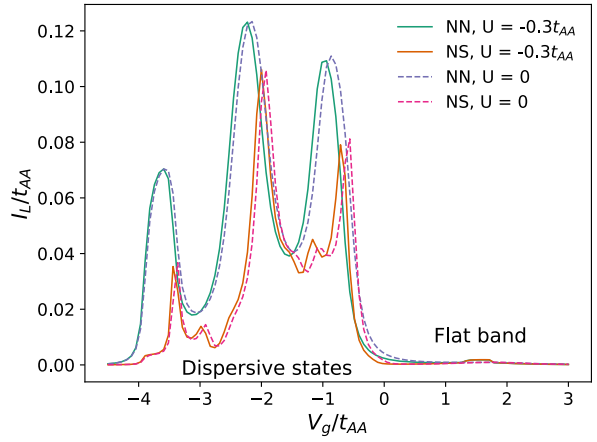


FIG. 3. Left lead current $I_L$ through the sawtooth lattice with three unit cells and an additional site in an NN and NS lead configuration at a varying gate potential $V_g$ with a constant bias $V$. The dispersive states correspond to peaks in the current. Flat-band states correspond to only very small peaks, in the presence of interactions, in both cases. The parameters are otherwise the same as in Fig. 2, but the order parameters are zero for the normal leads. Coherent pair transport does not contribute to the transport: In the NS configuration, the Andreev reflection is the only means for transport, since the bias $V$ is smaller than the superconducting order parameter amplitude $\Delta_R$, whereas in the NN case the usual transmission and reflection govern the transport. Even though the middle part acquires a finite order parameter due to the proximity effect, the superconducting order parameter phase is constant at the flat-band energy, and, thus, there is no coherent pair current. The small flat-band current contribution is due to the Hartree potential inhomogeneity.

mean-field theory, coherent pair current would require a superconducting order parameter phase gradient. In the case of the NN junction, the lack of pair transport processes is clear, since it turns out that the self-consistent order parameter at the sawtooth lattice vanishes. In the NS configuration, the phase of the order parameter there is found to be uniform even if the amplitude varies. Thus, there is no coherent pair current. The small flat-band current is caused by the Hartree potential inhomogeneity, which affects the destructive interference that causes localization, thereby enabling a quasiparticle current. It is remarkable that this Hartree-potential-induced quasiparticle current remains small, even at nonequilibrium. A sensitivity analysis for different ladder lengths as well as deviations from the perfect, disorder-free flat band and exact edge state degeneracy [43] shows that the flat-band state behavior observed here is robust.

Incoherent pair transport is not included in our mean-field theory approach. However, based on standard knowledge of superconducting junctions, it should be small. In a usual SS junction with a barrier between the superconductors characterized by a tunneling coupling $t$, the coherent pair transport (Josephson effect) is proportional to $t^2$, while incoherent pair tunneling is a process of the order of $t^4$, which for $t < 1$ is suppressed [61]. In our case, the inverse of the pair mass (determined by the interaction $|U|$) in the middle flat-band region gives effectively the tunneling coupling between the superconducting leads; it is small compared to the lead bandwidths. By analogy, it is then justified to first consider only the coherent pair transport. However, as flat bands have shown many surprises, it would be worthwhile to study in the future whether incoherent pair transport could be relevant, against expectations. Even if it is, the suppression of fermionic quasiparticle transport discovered here will have consequences to transport and device properties.

The system in Fig. 1 can be realized in ultracold gas two-terminal setups [22]. Our predictions can be tested there once low enough temperatures are reached to make the middle part superfluid, in addition to the leads [62,63]. One could also amend other ultracold gas platforms that demonstrated the Josephson effect [64–66]. In TBG devices, Josephson junctions can be defined by gate configurations on a single graphene bilayer [67–69]. For instance, SIS, SS′S, and SIS′IS junctions have been realized, where "S" is one type of superconductor and "S′" another and "I" denotes an insulating state. Close to our scenario are the two last ones, where S would be a superconductor in a part of the band that is maximally dispersive and S′ an area where the Fermi level is gated to match the flattest part of the band. One could also realize the desired junction by TBG material between superconducting leads.

In summary, we have shown by nonequilibrium self-consistent mean-field theory that coherent pair transport, i.e., the ac Josephson effect, largely dominates the flat-band

transport in a sawtooth ladder connected to superconducting leads. The transport in the dispersive band shows the usual behavior: ac Josephson current, as well as dc current realized via MAR. In contrast, quasiparticle transport is prominently absent in the flat-band case. With the leads in the NN and NS configurations, there is no current through the flat band, even when a small proximity-induced order parameter exists in the middle part. Again, this means that quasiparticle processes such as Andreev reflection are suppressed in the flat band. Equilibrium studies suggested quasiparticle localization for uniform systems of high symmetry [31,37]. It is remarkable that this is the case also in a *nonequilibrium* setting, with interfaces that could lead to complex processes akin to AR and MAR, and in a lattice where inhomogeneous Hartree potential combined with reduced symmetry may also induce transport.

So far, the main motivations of flat-band superconductivity studies have been high critical temperatures and strong correlations. Our results highlight that their *unique transport properties* make flat-band superconductors promising for quantum devices. In usual superconductors, there is always dissipation associated with ac currents at finite temperature due to quasiparticle current, termed as normal current in the two-fluid model [70]. This dissipation is present even at low frequencies and grows as frequency squared, limiting high-frequency operation. Our results indicate that quasiparticle transport (normal current) is quenched in a flat-band superconductor, and the dissipation related to it would be absent. This offers an intriguing prospect of *ultralow dissipation (low-power), high-frequency superconducting ac devices*. To evaluate this potential, one could start by reworking the Mattis-Bardeen theory [71] in the flat-band case. Flat-band superconductors might offer a "cure for quasiparticle poisoning"; quasiparticles, numerous at nonequilibrium even at low temperatures, limit the coherence of quantum bits based on Josephson junctions [72,73] and Majorana nanowires [74,75], lower the sensitivity of kinetic inductance detectors [76], and affect pumps, turnstiles, and microrefrigerators [73]. Our results suggest that a flat-band superconductor would block the transport of quasiparticles, even in a nonequilibrium situation, while letting supercurrent through. Thus, a flat-band-superconductor part could be used as a filter to block quasiparticles in the device, or the whole device could be built using flat-band superconductors. The latter requires developing a theory of Josephson junctions, Majorana wires, and superconducting devices based on flat-band superconductors.

P. T. and V. A. J. P. acknowledge support by the Academy of Finland under Projects No. 307419, No. 327293, and No. 349313. V. A. J. P. acknowledges financial support by the Jenny and Antti Wihuri Foundation. S. P. acknowledges support from the Academy of Finland under Grants No. 330384 and No. 336369.

*paivi.torma@aalto.fi

[1] D. Leykam, A. Andreanov, and S. Flach, Artificial flat band systems: From lattice models to experiments, Adv. Phys. **3**, 1473052 (2018).
[2] S. A. Parameswaran, R. Roy, and S. L. Sondhi, Fractional quantum Hall physics in topological flat bands, C.R. Phys. **14**, 816 (2013).
[3] E. J. Bergholtz and Z. Liu, Topological flat band models and fractional chern insulators, Int. J. Mod. Phys. B **27**, 1330017 (2013).
[4] Y. Cao, V. Fatemi, S. Fang, K. Watanabe, T. Taniguchi, E. Kaxiras, and P. Jarillo-Herrero, Unconventional superconductivity in magic-angle graphene superlattices, Nature (London) **556**, 43 (2018).
[5] A. H. MacDonald, Bilayer graphene's wicked, twisted road, Physics **12**, 12 (2019).
[6] E. Y. Andrei and A. H. MacDonald, Graphene bilayers with a twist, Nat. Mater. **19**, 1265 (2020).
[7] L. Balents, C. R. Dean, D. K. Efetov, and A. F. Young, Superconductivity and strong correlations in moiré flat bands, Nat. Phys. **16**, 725 (2020).
[8] D. M. Kennes, M. Claassen, L. Xian, A. Georges, A. J. Millis, J. Hone, C. R. Dean, D. N. Basov, A. N. Pasupathy, and A. Rubio, Moiré heterostructures as a condensed-matter quantum simulator, Nat. Phys. **17**, 155 (2021).
[9] E. Y. Andrei, D. K. Efetov, P. Jarillo-Herrero, A. H. MacDonald, K. F. Mak, T. Senthil, E. Tutuc, A. Yazdani, and A. F. Young, The marvels of moiré materials, Nat. Rev. Mater. **6**, 201 (2021).
[10] P. Törmä, S. Peotta, and B. A. Bernevig, Superconductivity, superfluidity and quantum geometry in twisted multilayer systems, Nat. Rev. Phys. **4**, 528 (2022).
[11] S. Peotta and P. Törmä, Superfluidity in topologically nontrivial flat bands, Nat. Commun. **6**, 8944 (2015).
[12] A. Julku, S. Peotta, T. I. Vanhala, D.-H. Kim, and P. Törmä, Geometric Origin of Superfluidity in the Lieb-Lattice Flat Band, Phys. Rev. Lett. **117**, 045303 (2016).
[13] L. Liang, T. I. Vanhala, S. Peotta, T. Siro, A. Harju, and P. Törmä, Band geometry, berry curvature, and superfluid weight, Phys. Rev. B **95**, 024515 (2017).
[14] P. Törmä, L. Liang, and S. Peotta, Quantum metric and effective mass of a two-body bound state in a flat band, Phys. Rev. B **98**, 220511(R) (2018).
[15] F. Xie, Z. Song, B. Lian, and B. A. Bernevig, Topology-Bounded Superfluid Weight in Twisted Bilayer Graphene, Phys. Rev. Lett. **124**, 167002 (2020).
[16] X. Hu, T. Hyart, D. I. Pikulin, and E. Rossi, Geometric and Conventional Contribution to the Superfluid Weight in Twisted Bilayer Graphene, Phys. Rev. Lett. **123**, 237002 (2019).
[17] A. Julku, T. J. Peltonen, L. Liang, T. T. Heikkilä, and P. Törmä, Superfluid weight and Berezinskii-Kosterlitz-Thouless transition temperature of twisted bilayer graphene, Phys. Rev. B **101**, 060505(R) (2020).
[18] M. Iskin, Origin of flat-band superfluidity on the Mielke checkerboard lattice, Phys. Rev. A **99**, 053608 (2019).
[19] M. Iskin, Two-body problem in a multiband lattice and the role of quantum geometry, Phys. Rev. A **103**, 053311 (2021).

[20] V. Peri, Z.-D. Song, B. A. Bernevig, and S. D. Huber, Fragile Topology and Flat-Band Superconductivity in the Strong-Coupling Regime, Phys. Rev. Lett. **126**, 027002 (2021).

[21] J. Herzog-Arbeitman, V. Peri, F. Schindler, S. D. Huber, and B. A. Bernevig, Superfluid Weight Bounds from Symmetry and Quantum Geometry in Flat Bands, Phys. Rev. Lett. **128**, 087002 (2022).

[22] V. A. J. Pyykkönen, S. Peotta, P. Fabritius, J. Mohan, T. Esslinger, and P. Törmä, Flat-band transport and Josephson effect through a finite-size sawtooth lattice, Phys. Rev. B **103**, 144519 (2021).

[23] K.-E. Huhtinen, J. Herzog-Arbeitman, A. Chew, B. A. Bernevig, and P. Törmä, Revisiting flat band superconductivity: Dependence on minimal quantum metric and band touchings, Phys. Rev. B **106**, 014518 (2022).

[24] S. M. Chan, B. Grémaud, and G. G. Batrouni, Pairing and superconductivity in quasi-one-dimensional flat-band systems: Creutz and sawtooth lattices, Phys. Rev. B **105**, 024502 (2022).

[25] S. M. Chan, B. Grémaud, and G. G. Batrouni, Designer flat bands: Topology and enhancement of superconductivity, Phys. Rev. B **106**, 104514 (2022).

[26] T. Kitamura, T. Yamashita, J. Ishizuka, A. Daido, and Y. Yanase, Superconductivity in monolayer FeSe enhanced by quantum geometry, Phys. Rev. Res. **4**, 023232 (2022).

[27] J. S. Hofmann, E. Berg, and D. Chowdhury, Superconductivity, pseudogap, and phase separation in topological flat bands, Phys. Rev. B **102**, 201112(R) (2020).

[28] Z. Wang, G. Chaudhary, Q. Chen, and K. Levin, Quantum geometric contributions to the BKT transition: Beyond mean field theory, Phys. Rev. B **102**, 184504 (2020).

[29] G. Orso and M. Singh, Pairs, trimers, and BCS-BEC crossover near a flat band: Sawtooth lattice, Phys. Rev. B **106**, 014504 (2022).

[30] M. Tovmasyan, S. Peotta, P. Törmä, and S. D. Huber, Effective theory and emergent SU(2) symmetry in the flat bands of attractive hubbard models, Phys. Rev. B **94**, 245149 (2016).

[31] J. Herzog-Arbeitman, A. Chew, K.-E. Huhtinen, P. Törmä, and B. A. Bernevig, Many-body superconductivity in topological flat bands, arXiv:2209.00007.

[32] T. T. Heikkilä, N. B. Kopnin, and G. E. Volovik, Flat bands in topological media, JETP Lett. **94**, 233 (2011).

[33] N. B. Kopnin, T. T. Heikkilä, and G. E. Volovik, High-temperature surface superconductivity in topological flat-band systems, Phys. Rev. B **83**, 220503(R) (2011).

[34] V. A. Khodel and V. R. Shaginyan, New approach in the microscopic fermi systems theory, Phys. Rep. **249**, 1 (1994).

[35] G. P. Parravicini and G. Grosso, *Solid State Physics* (Academic Press, New York, 2013).

[36] K. K. Likharev, *Dynamics of Josephson Junctions and Circuits* (Routledge, London, 2022).

[37] M. Tovmasyan, S. Peotta, L. Liang, P. Törmä, and S. D. Huber, Preformed pairs in flat Bloch bands, Phys. Rev. B **98**, 134513 (2018).

[38] H. Haug and A.-P. Jauho, *Quantum Kinetics in Transport and Optics of Semiconductors* (Springer, Berlin, 2008).

[39] G. Stefanucci and R. van Leeuwen, *Nonequilibrium Many-Body Theory of Quantum Systems: A Modern Introduction* (Cambridge University Press, Cambridge, England, 2013).

[40] J. Schwinger, Brownian motion of a quantum oscillator, J. Math. Phys. (N.Y.) **2**, 407 (1961).

[41] L. V. Keldysh, Diagram technique for nonequilibrium processes, Sov. Phys. JETP **20**, 1018 (1965).

[42] L. P. Kadanoff and G. Baym, *Quantum Statistical Mechanics* (Benjamin, New York, 1962).

[43] See Supplemental Material at http://link.aps.org/supplemental/10.1103/PhysRevLett.130.216003, which includes Refs. [44–51], for details of the model and the method, and a sensitivity analysis of the results to system parameter variations and imperfections.

[44] J. Rammer, *Quantum Field Theory of Non-Equilibrium States* (Cambridge University Press, Cambridge, England, 2007).

[45] G. Baym and L. P. Kadanoff, Conservation laws and correlation functions, Phys. Rev. **124**, 287 (1961).

[46] G. Baym, Self-consistent approximations in many-body systems, Phys. Rev. **127**, 1391 (1962).

[47] T. O. Espelid, Doubly adaptive quadrature routines based on Newton–Cotes rules, BIT **43**, 319 (2003).

[48] T. O. Espelid, Algorithm 868: Globally doubly adaptive quadrature—reliable Matlab codes, ACM Trans. Math. Softw. **33**, 21 (2007).

[49] D. G. Anderson, Iterative procedures for nonlinear integral equations, J. ACM **12**, 4 (1965).

[50] P. Pulay, Improved SCF convergence acceleration, J. Comput. Chem. **3**, 4 (1982).

[51] C. G. Broyden, A class of methods for solving nonlinear simultaneous equations, Math. Comput. **19**, 577 (1965).

[52] J. C. Cuevas, A. Martin-Rodero, and A. L. Yeyati, Hamiltonian approach to the transport properties of superconducting quantum point contacts, Phys. Rev. B **54**, 7366 (1996).

[53] A. Martín-Rodero and A. Levy Yeyati, Josephson and Andreev transport through quantum dots, Adv. Phys. **60**, 899 (2011).

[54] M. Alvarado and A. Levy Yeyati, Transport and spectral properties of magic-angle twisted bilayer graphene junctions based on local orbital models, Phys. Rev. B **104**, 075406 (2021).

[55] A.-P. Jauho, N. S. Wingreen, and Y. Meir, Time-dependent transport in interacting and noninteracting resonant-tunneling systems, Phys. Rev. B **50**, 5528 (1994).

[56] G. E. Blonder, M. Tinkham, and T. M. Klapwijk, Transition from metallic to tunneling regimes in superconducting microconstrictions: Excess current, charge imbalance, and supercurrent conversion, Phys. Rev. B **25**, 4515 (1982).

[57] S. Datta, P. F. Bagwell, and M. P. Anantram, Scattering theory of transport for mesoscopic superconductors, technical report, Purdue University, 1996.

[58] A. F. Andreev, Thermal conductivity of the intermediate state in superconductors, Sov. Phys. JETP **19**, 1228 (1964).

[59] T. M. Klapwijk, G. E. Blonder, and M. Tinkham, Explanation of subharmonic energy gap structure in superconducting contacts, Physica (Amsterdam) **109-110B+C**, 1657 (1982).

[60] B. D. Josephson, Possible new effects in superconductive tunneling, Phys. Lett. **1**, 7 (1962).

[61] G. D. Mahan, *Many-Particle Physics*, 3rd ed. (Springer, New York, 2000).
[62] D. Husmann, S. Uchino, S. Krinner, M. Lebrat, T. Giamarchi, T. Esslinger, and J.-P. Brantut, Connecting strongly correlated superfluids by a quantum point contact, Science **350**, 1498 (2015).
[63] M.-Z. Huang, J. Mohan, A.-M. Visuri, P. Fabritius, M. Talebi, S. Wili, S. Uchino, T. Giamarchi, and T. Esslinger, Superfluid current through a dissipative quantum point contact, arXiv:2210.03371 [Phys. Rev. Lett. (to be published)].
[64] M. Albiez, R. Gati, J. Fölling, S. Hunsmann, M. Cristiani, and M. K. Oberthaler, Direct Observation of Tunneling and Nonlinear Self-Trapping in a Single Bosonic Josephson Junction, Phys. Rev. Lett. **95**, 010402 (2005).
[65] G. Valtolina, A. Burchianti, A. Amico, E. Neri, K. Xhani, J. A. Seman, A. Trombettoni, A. Smerzi, M. Zaccanti, M. Inguscio, and G. Roati, Josephson effect in fermionic superfluids across the BEC-BCS crossover, Science **350**, 1505 (2015).
[66] N. Luick, L. Sobirey, M. Bohlen, V. P. Singh, L. Mathey, T. Lompe, and H. Moritz, An ideal Josephson junction in an ultracold two-dimensional Fermi gas, Science **369**, 89 (2020).
[67] F. K. de Vries, E. Portolés, G. Zheng, T. Taniguchi, K. Watanabe, T. Ihn, K. Ensslin, and P. Rickhaus, Gate-defined Josephson junctions in magic-angle twisted bilayer graphene, Nat. Nanotechnol. **16**, 760 (2021).
[68] D. Rodan-Legrain, Y. Cao, J. M. Park, S. C. de la Barrera, M. T. Randeria, K. Watanabe, T. Taniguchi, and P. Jarillo-Herrero, Highly tunable junctions and non-local Josephson effect in magic-angle graphene tunnelling devices, Nat. Nanotechnol. **16**, 769 (2021).
[69] J. Diez-Merida, A. Diez-Carlon, S. Y. Yang, Y. M. Xie, X. J. Gao, K. Watanabe, T. Taniguchi, X. Lu, K. T. Law, and D. K. Efetov, Magnetic Josephson junctions and superconducting diodes in magic angle twisted bilayer graphene, arXiv:2110.01067.
[70] M. Tinkham, *Introduction to Superconductivity*, 2nd ed. (Dover Publications, Mineola, NY, 2004).
[71] D. C. Mattis and J. Bardeen, Theory of the anomalous skin effect in normal and superconducting metals, Phys. Rev. **111**, 412 (1958).
[72] J. Aumentado, M. W. Keller, J. M. Martinis, and M. H. Devoret, Nonequilibrium Quasiparticles and 2*e* Periodicity in Single-Cooper-Pair Transistors, Phys. Rev. Lett. **92**, 066802 (2004).
[73] G. Catelani and J. P. Pekola, Using materials for quasiparticle engineering, Mater. Quantum Technol. **2**, 013001 (2022).
[74] D. Rainis and D. Loss, Majorana qubit decoherence by quasiparticle poisoning, Phys. Rev. B **85**, 174533 (2012).
[75] A. P. Higginbotham, S. M. Albrecht, G. Kiršanskas, W. Chang, F. Kuemmeth, P. Krogstrup, T. S. Jespersen, J. Nygård, K. Flensberg, and C. M. Marcus, Parity lifetime of bound states in a proximitized semiconductor nanowire, Nat. Phys. **11**, 1017 (2015).
[76] P. J. de Visser, J. J. A. Baselmans, P. Diener, S. J. C. Yates, A. Endo, and T. M. Klapwijk, Generation-recombination noise: The fundamental sensitivity limit for kinetic inductance detectors, J. Low Temp. Phys. **167**, 335 (2012).